

REPORT



Host cell protein detection gap risk mitigation: quantitative IAC-MS for ELISA antibody reagent coverage determination

Daniel M. Waldera-Lupa^a, Yvonne Jasper^a, Pia Köhne^a, Ronja Schwichtenhövel^a, Heiner Falkenberg^a, Thomas Flad^a, Peter Happersberger^b, Bernd Reisinger^b, Alireza Dehghani^b, Roland Moussa^a, and Thomas Waerner^b

^aBioanalytics, Protagen Protein Services GmbH, Dortmund, Germany; ^bAnalytical Development Biologicals, Boehringer Ingelheim Pharma GmbH & Co. KG, Biberach, Germany

ABSTRACT

Host cell proteins (HCPs) must be sufficiently cleared from recombinant biopharmaceuticals during the downstream process (DSP) to ensure product quality, purity, and patient safety. For monitoring of HCP clearance, the typical method chosen is an enzyme-linked immunosorbent assay (ELISA) using polyclonal anti-HCP antibodies obtained from an immunization campaign. This polyclonal reagent is a critical factor for functionality and confidence of the ELISA. Therefore, it is important to ensure that the pool of ELISA antibodies covers a broad spectrum of the HCPs that potentially could persist in the final drug substance. Typically, coverage is determined by gel-based approaches. Here, we present a quantitative proteomics approach combined with purification of HCPs by immunoaffinity chromatography (qIAC-MS) for assessment of ELISA coverage. The cell culture fluid (CCF) of a mock fermentation and a recombinant monoclonal antibody product were characterized in detail to investigate whether the HCPs used for immunization of animals accurately represent HCPs that are relevant to the process. Using the qIAC-MS approach, the ELISA antibody coverage was determined for mock fermentation and product CCF, as well as several different DSP intermediates. Here, the use of different controls facilitated the identification and quantification of HCPs present in the polyclonal reagent and those that nonspecifically bound to IAC material. This study successfully demonstrates that the described qIAC-MS approach is not only a suitable orthogonal method to commonly used 2D SDS-PAGE-based analysis for evaluating ELISA antibody coverage, but that it further identifies HCPs covered as well as missed by the ELISA, enabling an improved risk assessment of HCP ELISA.

ARTICLE HISTORY

Received 29 March 2021
Revised 17 June 2021
Accepted 9 July 2021

KEYWORDS

Host cell protein; mass spectrometry; proteomics; biopharmaceuticals; ELISA coverage; affinity purification; immunoprecipitation; HCP; IAC; qIAC-MS; immunoaffinity chromatography

Introduction

Host cell proteins (HCPs) are low-level process-related impurities that must be adequately cleared from recombinant biopharmaceuticals during the downstream process (DSP) to ensure product quality, purity, and patient safety.^{1,2} HCPs are regarded as a critical quality attribute (CQA) in biopharmaceuticals due to potential immunogenicity risks for patients,³ constraints on drug efficacy *in vivo*,⁴ and negative impacts on product quality,^{5–7} including formulation components.^{8,9} As such, they must be analyzed using sensitive detection methods and quantified throughout the DSP and in the final drug substance (DS).


The typical, current approach for monitoring HCP clearance during process development and release testing uses an enzyme-linked immunosorbent assay (ELISA) because of its high throughput, sensitivity, and selectivity.¹⁰ Polyclonal anti-HCP antibodies, collectively referred to as the anti-HCP-Ab, obtained from an immunization campaign are a critical component of the assay. It is important to ensure that the anti-HCP-Ab for ELISA covers a broad spectrum of the HCPs that potentially could remain in the final DS.¹¹ Due to low immunoreactivity of some HCPs during immunization, some HCPs

may not be recognized by the anti-HCP-Ab, as antibodies are only generated against immunocompetent HCPs. Furthermore, some HCPs may not be detected by the anti-HCP-Ab due to low antibody affinity or low availability of HCP epitopes. Therefore, it is necessary to identify the covered and non-covered HCPs and to determine the anti-HCP antibody coverage before product marketing.

Typically, the ELISA antibody coverage is determined by gel-based approaches such as two-dimensional polyacrylamide gel electrophoresis (2D-PAGE) or 2D-Western blotting.¹² Here, the spot pattern of the 2D-PAGE is compared to a 2D-Western blot with the anti-HCP-Ab as the primary antibody reagent. Gel-based approaches have inherent limitations, such as potentially incomplete HCP resolution, complex spot patterns resulting from different modifications of the same HCP producing several spots, incomplete transfer to the blotting membrane, denaturing of native epitopes during 2D-PAGE, reliance on visual comparison, and no simultaneous identification of HCPs.^{12–16} Thus, more reliable and accurate approaches are needed for detailed characterization of ELISA antibody coverage.

Mass spectrometry (MS) is increasingly used for the identification and quantification of process-related HCP impurities

CONTACT Thomas Waerner  thomas.waerner@boehringer-ingelheim.com  Analytical Development Biologicals, Boehringer Ingelheim Pharma GmbH & Co. KG, Birkendorfer Strasse 65, Biberach an der Riss, Biberach 88397, Germany

 Supplemental data for this article can be accessed on the [publisher's website](#)

© 2021 The Author(s). Published with license by Taylor & Francis Group, LLC.

This is an Open Access article distributed under the terms of the Creative Commons Attribution-NonCommercial License (<http://creativecommons.org/licenses/by-nc/4.0/>), which permits unrestricted non-commercial use, distribution, and reproduction in any medium, provided the original work is properly cited.

by quantitative proteomics. Recent proteomics studies have demonstrated sensitive detection for the identification of low-abundance HCPs in purified DS^{17–22} and for the characterization of upstream and downstream process influences on resulting HCP patterns for different recombinant monoclonal antibody (mAb) products.²³ During the DSP, MS technology is capable of detecting individual HCPs, which is needed for thorough understanding of the process. This detailed characterization is particularly helpful for process optimization, which is achieved by monitoring persistence and depletion of individual HCPs that may pose an increased level of risk.²⁴ Thus, MS is a valuable method for monitoring HCP clearance during process development, and its use significantly improves risk assessment in HCP control.²⁵

Affinity purification by immunoaffinity chromatography (IAC) coupled to MS is a selective and sensitive approach for isolation and identification of binding partners to a specific target protein and is widely used for the discovery of protein–protein interactions.^{26,27} This approach, however, also can be used for evaluating more complex mixtures, as done herein for the determination of ELISA antibody coverage. In this application, the target protein is a mixture of polyclonal antibodies (anti-HCP-Ab), and the binding partner is a complex and heterogeneous mixture of a broad spectrum of different HCPs. Factors like antibody titers, antigen-binding affinities, and immunogenic HCP concentrations influence the results, and therefore have to be considered. IAC-MS for ELISA antibody coverage determination can be challenging, and appropriate controls are needed to generate high-confidence results. Recently, two MS-based approaches were described for the determination of ELISA antibody coverage.^{28,29} Both approaches show high sensitivity to identification and quantification of HCPs by MS. Moreover, it was shown that IAC-MS overcomes some limitations of gel-based approaches. However, the approaches described require biotinylation of the anti-HCP-Ab for coupling, and the quantification strategies used do not allow mapping of identifications between the different samples, which is necessary for the unambiguous determination of specifically and nonspecifically bound HCPs. It also remains untested whether these published approaches are suitable for determining the coverage for samples containing active pharmaceutical ingredient (API), as it was tested only for the analysis of mock fermentations without high abundant API.

In this study, a quantitative IAC-MS (qIAC-MS) approach using label-free quantification was applied to analyze anti-HCP-Ab-enriched HCPs. First, non-enriched samples of cell culture fluid (CCF) from a mock fermentation (a transfected cell line without the drug product) and corresponding drug product (CCF of the cell line containing the drug product) were characterized quantitatively by standard LC-MS approach to define the HCP pool and further investigate whether HCPs used for animal immunization accurately represent HCPs that are relevant for the process. Subsequently, the developed qIAC-MS approach was performed on the same mock fermentation and CCF samples of the representative mAb manufacturing along with a set of DSP samples, consisting of five different purification intermediates. Selected controls allow the identification and quantification of HCPs present in the anti-HCP-Ab-

enriched sample (target contaminants) and to distinguish non-specifically bound to the IAC material. Using this method, the ELISA antibody coverage was determined for each purification step, and the results were compared to coverage analysis determined by applying 2D-PAGE and 2D-Western blot.

The qIAC-MS approach described here is characterized by direct coupling of the anti-HCP-Ab to magnetic particles and a label-free quantification strategy enabling the determination of specifically and nonspecifically bound HCPs. Since identifications are mapped between the samples, this approach also enables the classification of HCPs with lower abundance. Moreover, the approach is deemed as applicable for the analysis of process samples containing highly abundant API. This qIAC-MS approach has proven so valuable for product development, and particularly characterization of HCP ELISA, that Boehringer Ingelheim now routinely uses it across new product developments, respective processes and for implementation into dossiers for New Biological Entities (NBE). The collected data is being compiled into a database and digitized so that we might ultimately achieve generalizable understanding of HCP profiles over the whole production and purification process to further improve understanding and control of HCP levels for development of new biopharmaceutical products.

Results

Anti-HCP ELISA is the current gold standard for monitoring HCP clearance during process development, as well as for final product release testing. It enables robust and high-throughput quantification of residual HCP levels. However, ELISA does not allow quantification and identification of individual HCPs. For quality testing of clinical and commercial products by ELISA, it is therefore essential to ensure that the anti-HCP-Ab recognizes a broad spectrum of the HCPs that occur in the bioprocess.¹ This is especially true for putative, high-risk HCPs, which are potentially immunogenic or product degrading, because their detection is mandatory. For this reason, the anti-HCP-Ab coverage is usually determined to demonstrate suitability of the ELISA for a specific bioprocess before bringing the product to the market. Here, a quantitative IAC approach suitable to detect very low levels of HCP using IAC enrichment combined with mass spectrometry (qIAC-MS) is described for detailed and efficient ELISA antibody coverage determination. Applying the qIAC-MS approach, the cell culture fluid (CCF) of a mock fermentation (Mock CCF; a transfected cell line without the drug product), the CCF of the cell line containing the drug product (Product CCF), and five different samples of the DSP, including capture pool (CP, Protein A purification), depth filter pool (DFP), polishing #1 pool (Pol1), polishing #2 pool (Pol2), and ultrafiltration/diafiltration (UFDF), were analyzed.

Characterization of HCP immunogen and Product CCF by standard LC-MS

The HCP immunogen is an important factor in generating an anti-HCP ELISA. Usually, immunogen is taken from CCF of a mock fermentation because it contains as many HCPs as possible that are relevant for the process. As a baseline for

comparison of the new qIAC-MS approach, a standard LC-MS approach was used to investigate whether HCPs derived from the CCF of mock fermentation represent HCPs that are present in the mAb production process (represented by the so-called “Product CCF”) and to compare the physicochemical properties (molecular weight (MW) and isoelectric point (pI)) of underlying HCPs by depiction in a virtual 2D gel image.

Using a standard LC-MS approach without enrichment, 1073 HCPs were identified in total in the Mock CCF and Product CCF samples. The majority of HCPs (821 HCPs, 76.5%) were identified in both samples, whereas 220 HCPs (20.5%) were uniquely identified in the Mock CCF and only 32 HCPs (3.0%) solely in the Product CCF sample (Figure 1a). Thus, both samples showed a high degree of similarity in HCP species. The Mock CCF analyzed within this study had an expanded fermentation time to increase the total level of HCPs. The utility of this approach is that some HCPs become concentrated above the detection level, but, on the other hand, some HCPs may be present in the Mock CCF only due to the extended fermentation time and may not be representative of HCPs in the Product CCF. The entire HCP pool of Mock and Product CCFs detected by LC-MS analysis spanned theoretical MWs from 5 to 585 kDa and a theoretical pI range of 4–12 (Figure 1b). The majority of HCPs had a theoretical MW \leq 75 kDa (72.7%) with a maximum around \sim 50 kDa and a pI $<$ 8 (63.1%) with a maximum between pI 6 and 7. Comparison of HCPs uniquely identified in Mock (220 HCPs) or Product CCF (32 HCPs) revealed no apparent differences either in MW (median Mock: 44.7 kDa; median CCF: 46.9 kDa) or in pI range (median Mock: 6.4; median CCF: 6.6) (Figure 1c).

Next, Mock and Product CCFs were compared using quantitative LC-MS data. Correlation analysis using individual HCP abundances in Mock and Product CCFs resulted in a heterogeneous abundance distribution between both samples with a Pearson correlation coefficient of 0.64 (Figure 1d). By LC-MS analysis, most of the HCPs showed a comparable abundance in both samples, whereas 7.9% (65 HCPs) showed a high abundance in Mock and a low abundance in Product CCF, and only 3.9% (32 HCPs) had the opposite distribution with a high level in Product CCF and a low level in Mock CCF. All HCPs uniquely identified either in Mock CCF or in Product CCF were found solely in low abundance compared to the mean abundance of all identified HCPs of the respective sample. In a virtual 2D plot of MW and pI, where spot size is scaled according to relative abundance, both samples showed a slightly different abundance distribution, albeit most of the HCPs exhibited a comparable abundance (Figure 1e). This becomes clearer when the ratio of individual HCP abundance between Mock CCF and Product CCF is plotted (Figure 1f). Here, basic proteins or proteins with a lower MW were more strongly represented in Product CCF.

IAC of HCP immunogen and Product CCF

For many years, IAC has been a valuable tool for the enrichment of proteins in the scientific research environment.^{26,27} Here, this technology was implemented for the characterization of anti-HCP polyclonal antibodies (anti-HCP-Ab), a critical reagent for ELISA-based detection of HCPs in

biopharmaceutical products during release testing. It should be noted that IAC-MS analysis for establishing ELISA antibody coverage determination can be challenging and appropriate controls are needed to generate high-confidence results. Therefore, in this study, the IAC method was extensively optimized, and a quantitative approach (qIAC-MS) using negative controls was established, as depicted in the analytical workflow of the study (Figure 2). Two different negative controls were used in the qIAC-MS approach: (1) HCPs identified within the Bead Control (BC, coupled anti-HCP-Ab without antigen; top panel of Figure 2); and (2) HCPs that showed a higher or similar abundance in the Negative Control (NC, antigen without coupled anti-HCP-Ab; bottom panel of Figure 2). The results of the NC were compared to the IAC antigen sample and those that bound at a higher level in the NC ($NC \geq IAC$) were excluded from further evaluation, as they are seen as an artifact of the method and are not reflective of the product’s HCP pool. The HCPs identified in BC also were not included because these species are contaminants from the anti-HCP-Ab reagent.

First, qIAC-MS was applied separately to Mock CCF and Product CCF samples to investigate whether the presence of the API in Product CCF has an impact on HCP detection compared to Mock CCF, which does not contain any API. A total of 821 HCPs were identified in qIAC-MS of Mock CCF (Figure 3a) and 605 HCPs in qIAC-MS of Product CCF (Figure 3b) (Table 1). Comparison of the qIAC-MS results with the standard LC-MS data revealed an overlap of 83.6% (799 HCPs) for Mock and 68.3% (570 HCPs) for Product CCFs. However, 135 HCPs (14.1%) and 230 HCPs (27.5%) were uniquely detected in the LC-MS data of Mock CCF and Product CCF, respectively, that were not detected by qIAC-MS analysis. This indicates that the presence of the API in Product CCF has an impact on the IAC-enrichment and/or the HCP detection by MS.

To better understand the meaning of the difference in coverage between the two samples, the standard LC-MS and qIAC-MS data were compared quantitatively. Correlation analysis using quantitative data revealed a strong correlation between LC-MS and qIAC-MS of Mock CCF ($r=0.80$) (Figure 3c), and a slightly less strong correlation between LC-MS and qIAC-MS of Product CCF ($r=0.72$) (Figure 3d). The majority of HCPs showed comparable abundances by LC-MS and qIAC-MS analysis, whereas HCPs uniquely detected by one analysis type were observed at low abundance compared to the mean abundance of the respective sample. The 2D plots (MW and pI) of HCPs detected by the different methods showed similar results for the Mock (Figure 3e) and Product CCF samples (Figure 3f). The high-abundance HCPs were distributed over the entire theoretical MW and pI ranges, whereas only a few individual HCPs showed a significant difference in abundance between the two methods. Most of the HCPs that were not detected by qIAC-MS (unique in LC-MS analysis) exhibited a lower theoretical MW and were distributed over the whole pI range. Accordingly, use of the anti-HCP-Ab to enrich HCPs in the samples appears to enrich the HCPs in both matrices, such that an effect can be recognized due to the presence or absence of the API.

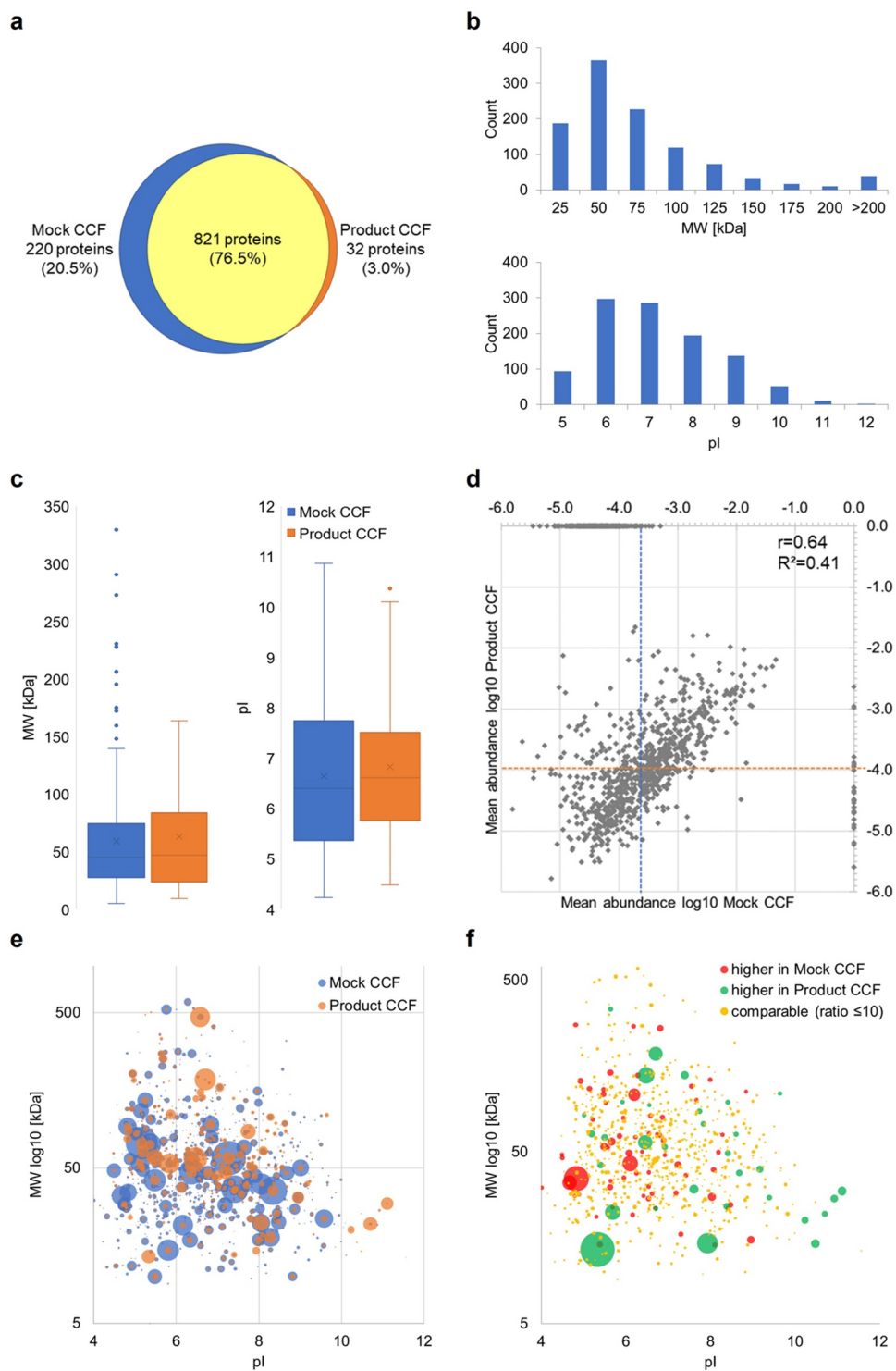


Figure 1. Comparison of HCP pattern of Mock CCF and Product CCF analyzed by standard LC-MS. (a) Venn diagram of Mock (blue) compared to HCPs identified in Product CCF (orange). (b) Histogram of MW (kDa) and pI of proteins identified in Mock and Product CCF. (c) Box-plot of MW (kDa) and pI of proteins uniquely identified in Mock or Product CCF. (d) Scatter plot of identified HCPs with the corresponding Pearson correlation coefficient ($r=0.64$) and coefficient of determination ($R^2=0.41$). For each condition, the log₁₀ intensity is shown. The dots on the axis represent HCPs uniquely identified in one sample (x-axis: Mock CCF (220 proteins), y-axis: Product CCF (32 proteins)). The dotted lines represent the mean abundance of all proteins for the specific sample (blue: Mock CCF, orange: Product CCF). (e) 2D-plot (pI and MW) of proteins identified in Mock CCF (blue) or Product CCF (orange). The spot size represents the relative protein abundance. (f) 2D-plot (pI and MW) of proteins identified in both samples. The spot size represents the ratio between both samples (higher in Mock CCF: red; higher in Product CCF: green; comparable abundance (ratio ≤ 10): yellow).

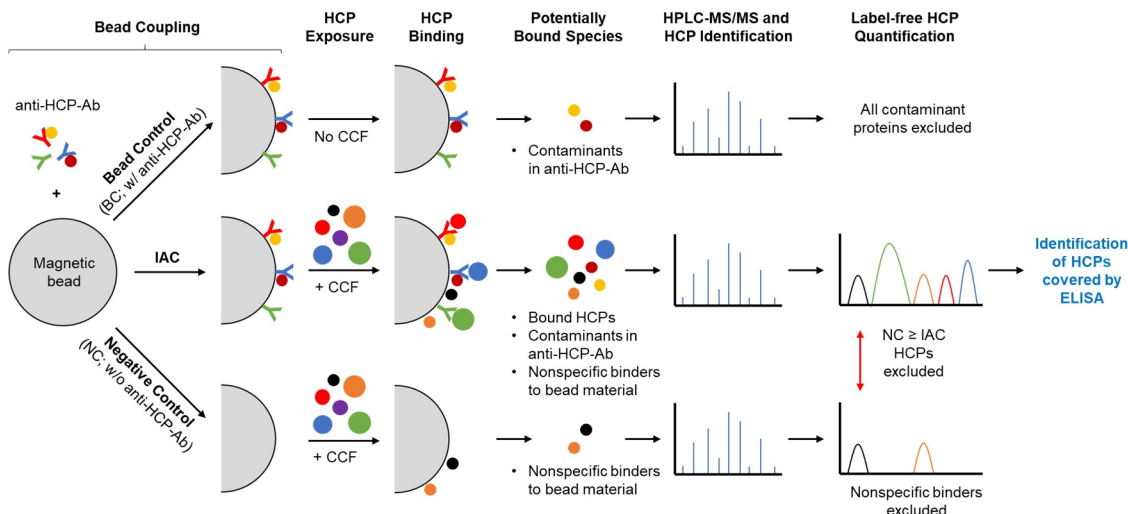


Figure 2. Schematic representation of the developed qIAC-MS approach for ELISA antibody coverage determination. Three separate analyses were conducted using the bead material. As shown in the top panel for the Bead Control (BC), the bead material was coupled with anti-HCP-Ab but not exposed to CCF and the eluate was analyzed to identify any protein contaminants in the ELISA reagent. The middle panel shows the experimental IAC, where the coupled beads are exposed to CCF and the resulting data includes HCPs as well as the ELISA reagent contaminants and nonspecific binders. The bottom panel depicts the Negative Control (NC), which utilized beads that had not been coupled with anti-HCP-Ab and were exposed to CCF to identify nonspecific binders, which were eliminated from the HCP analysis depending upon the relative level compared to IAC. Combining the three analyses results in identification of HCPs that are bound by the anti-HCP-Ab ELISA reagent.

IAC of downstream process intermediates

Purification of the mAb product and robust HCP clearance are crucial steps in the whole production process.^{13–15} Monitoring of residual HCPs by ELISA is indispensable for quality control and risk assessment.^{1,2,25} Therefore, it is highly relevant that the ELISA antibody reagent provides sufficient coverage of the HCPs throughout the whole DSP, as different sample conditions can influence detection. For this reason, the ELISA antibody reagent was investigated further to assess how well it recognizes the HCPs in different steps of the DSP.

Altogether, 839 HCPs were considered for evaluation of the DSP (Table 1). As expected, the majority of HCPs were identified in Product CCF. A significant decrease of HCPs was measured after the first purification step (CP: Protein A purification), and a further depletion was seen along the DSP (Figure 4a). Compared to Product CCF, where more HCPs were identified by the standard LC-MS method than by qIAC-MS (ratio 0.8), the later DSP samples showed an enrichment of HCPs by IAC compared to LC-MS detection (ratios: 1.3–2.0) (Table 1). Thus, the IAC is able to enrich a panel of low abundant HCPs in the less complex intermediates.

Next, we compared the distribution of HCPs among the DSP samples enriched by IAC. A total of 35 HCPs (5.5%) were detected in all six DSP intermediates and only a low number of HCPs were unique for any specific intermediate, except Product CCF, where the majority of HCPs were identified (Figure 4b). When comparing only the purified samples (without CCF) more than two-thirds of the HCPs (232 HCPs, 71.2%) were detected in at least two DSP samples and 94 HCPs (28.8%) were detected in only one sample (Figure 4c). This indicates that all DSP samples were homogeneously enriched by IAC.

In addition, the total number of identified HCPs in DSP detected by the standard LC-MS and qIAC-MS approaches was compared. In this analysis, 642 HCPs were identified by qIAC-MS of DSP, whereas 197 HCPs (23.5%) were uniquely identified by LC-MS of DSP and 38 HCPs (4.5%) uniquely

by qIAC-MS (Figure 4d). Comparison of the HCPs that were uniquely identified by LC-MS of DSP with results of qIAC-MS of Mock CCF revealed that the majority (128 HCPs, 65.0%) of HCPs were identified by qIAC-MS of Mock, and therefore enriched by IAC with the anti-HCP-Ab (Supplementary Fig. 1a). However, 69 HCPs identified by LC-MS of DSP did not appear to be enriched by the ELISA antibody (8.2% of 839 HCPs of all HCPs detected during the whole DSP). Of these 69, 52 HCPs also were identified by LC-MS of Mock CCF, and only 17 HCPs were uniquely detected by LC-MS of DSP (Supplementary Fig. 1b). Thus, the majority (76.5%) of HCPs in the DSP intermediates were enriched by IAC with the anti-HCP-Ab, yet nearly a quarter of the HCP pool was not, indicating ELISA coverage of these impurities may be less than optimal. The results we obtained from this approach are valuable for improved understanding of the product-specific ELISA performance.

Physicochemical properties of IAC-enriched HCPs

To investigate whether IAC has a bias for the enrichment of specific HCPs, the IAC-enriched and non-enriched HCPs of Mock CCF, Product CCF, and DSP intermediates were characterized to establish their relative abundance (spectral counting by peptide spectrum matches; PSMs) and assess differences with respect to physicochemical properties (MW and pI). The HCPs identified by both approaches (16 PSMs) showed a higher abundance compared to the uniquely identified HCPs (MS: 4 PSMs; qIAC-MS: 3 PSMs) (Figure 5a). Assessment of the theoretical MW for these species revealed a decrease in HCPs below 25 kDa and an increase in HCPs with higher MW (>150 kDa) with the qIAC-MS approach compared to standard LC-MS (Figure 5b). Evaluation of the theoretical pI range revealed fewer acidic species, and no HCPs above pI 9 were detected

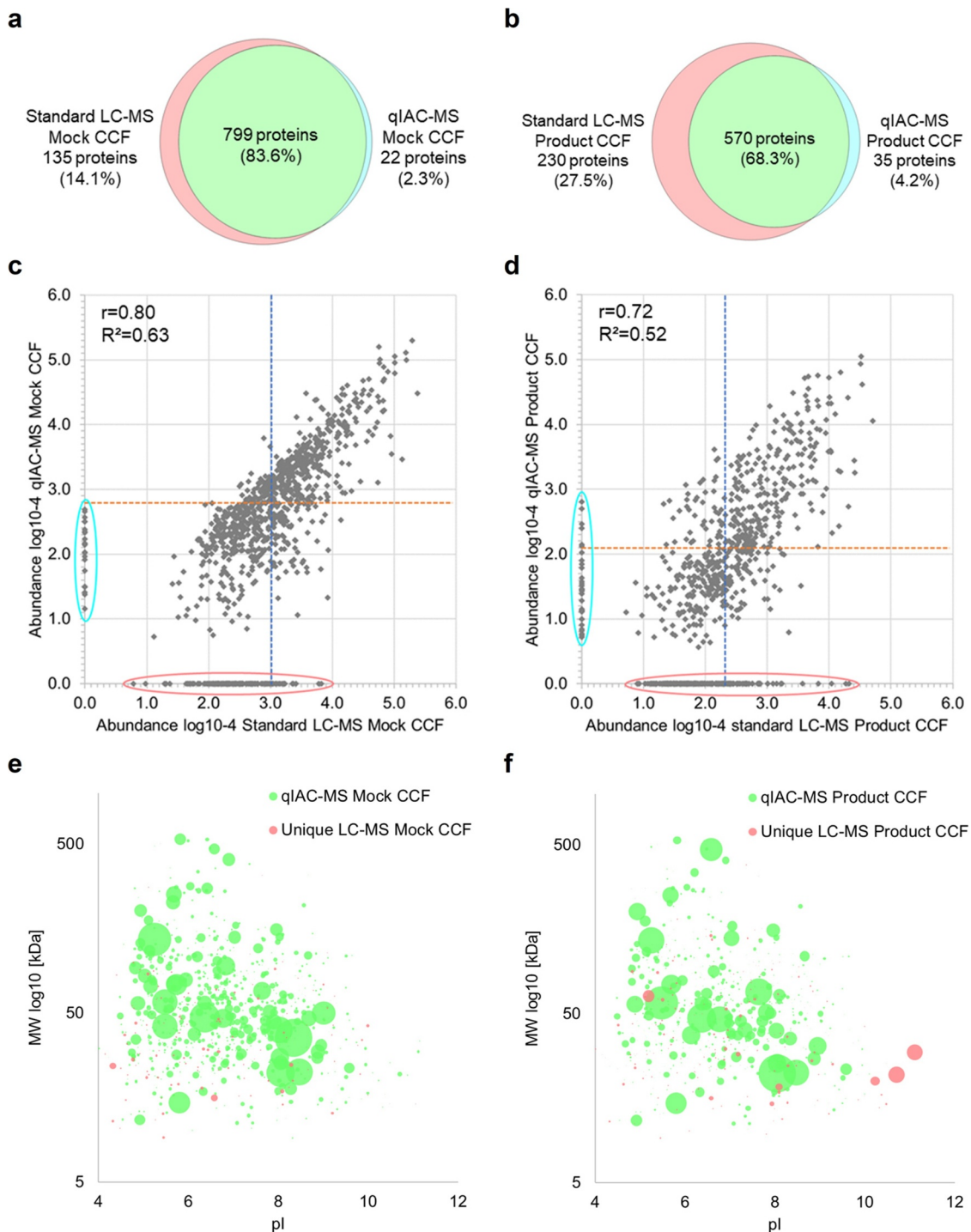


Figure 3. Comparison of standard LC-MS and qIAC-MS data of Mock and Product CCF. For qIAC-MS approach, HCPs that showed a higher or similar abundance in the Negative Control compared to the IAC antigen sample ($NC \geq IAC$) were not considered for visualization. (a) Venn diagram of standard LC-MS of Mock CCF (red) compared to qIAC-MS of Mock CCF (cyan). (b) Venn diagram of standard LC-MS Product CCF (red) compared to qIAC-MS of Product CCF (cyan). (c,d) Scatter plot of identified HCPs in Mock CCF (c) and Product CCF (d) sample with the corresponding Pearson correlation coefficient (Mock CCF: $r=0.80$; Product CCF: $r=0.72$) and coefficient of determination (Mock CCF: $R^2=0.63$; Product CCF: $R^2=0.52$). For each condition the \log_{10} intensity is shown. The dotted lines represent the mean abundance of all HCPs for the specific sample (blue: Mock CCF or Product CCF, orange: qIAC-MS of Mock CCF or qIAC-MS of Product CCF). HCPs uniquely identified standard LC-MS or qIAC-MS are circled (red: Mock CCF or Product CCF, cyan: qIAC-MS of Mock CCF or qIAC-MS of Product CCF) (e,f) 2D-plot (pI and MW) of HCPs identified in qIAC-MS of Mock CCF (e) or qIAC-MS of Product CCF (f). The spot size represents the relative protein abundance. HCPs uniquely identified in standard LC-MS analysis are shown in red.

by the qIAC-MS approach (Figure 5c). However, it must be considered that due to the low number of HCPs uniquely detected by qIAC-MS, no valid statistical assessment could be made to establish significance of these differences in MW and pI distribution.

Determination of ELISA antibody coverage

As demonstrated above, the applied qIAC-MS approach is able to enrich, identify, and quantify HCPs from process samples. Next, the ELISA antibody coverage for Mock

Table 1. Results of IAC-enrichment of Mock fermentation (Mock CCF), product cell culture fluid (CCF; Product CCF), and DSP intermediates (capture pool (CP), depth filter pool (DFP), polishing 1 (Pol1), polishing 2 (Pol2), ultrafiltration/diafiltration (UFDF)).

Sample	HCPs Identified in standard LC-MS	HCPs Identified in qIAC-MS	Ratio qIAC-MS / standard LC-MS
Mock CCF	934	821	0.9
Product CCF	800	605	0.8
CP	150	195	1.3
DFP	112	173	1.5
Pol1	91	156	1.7
Pol2	83	166	2.0
UFDF	86	143	1.6

fermentation, Product CCF, and the DSP intermediates was determined. In order to obtain a highly reliable determination of specifically and nonspecifically bound HCPs, an appropriate threshold for the difference in abundance between IAC (antigen with anti-HCP-Ab) and NC (antigen without anti-HCP-Ab) was defined. Therefore, the

variability of the applied label-free quantification approach (20%–50%)^{30–32} was taken into account, and four different levels of stringency in evaluating the HCP data for the NC were set and compared. Here, thresholds for the difference in abundance (fold change) of IAC to NC were set with increasing stringency, and HCPs with 1-fold (no variability considered); 1.5-fold (50% variability considered); 2-fold (100% variability considered); or 5-fold (500% variability considered) lower or equal abundance in the IAC antigen sample compared to the NC were not considered as enriched, and therefore not counted as positive for coverage determination at that stringency level. Furthermore, for calculation of the coverage, either the HCPs identified in the intersection of standard LC-MS and qIAC-MS (overlapping HCPs divided by all HCPs detected in standard LC-MS) or the total number of HCPs identified in qIAC-MS (all HCPs detected in qIAC-MS divided by all HCPs detected in standard LC-MS) was used. For the latter,

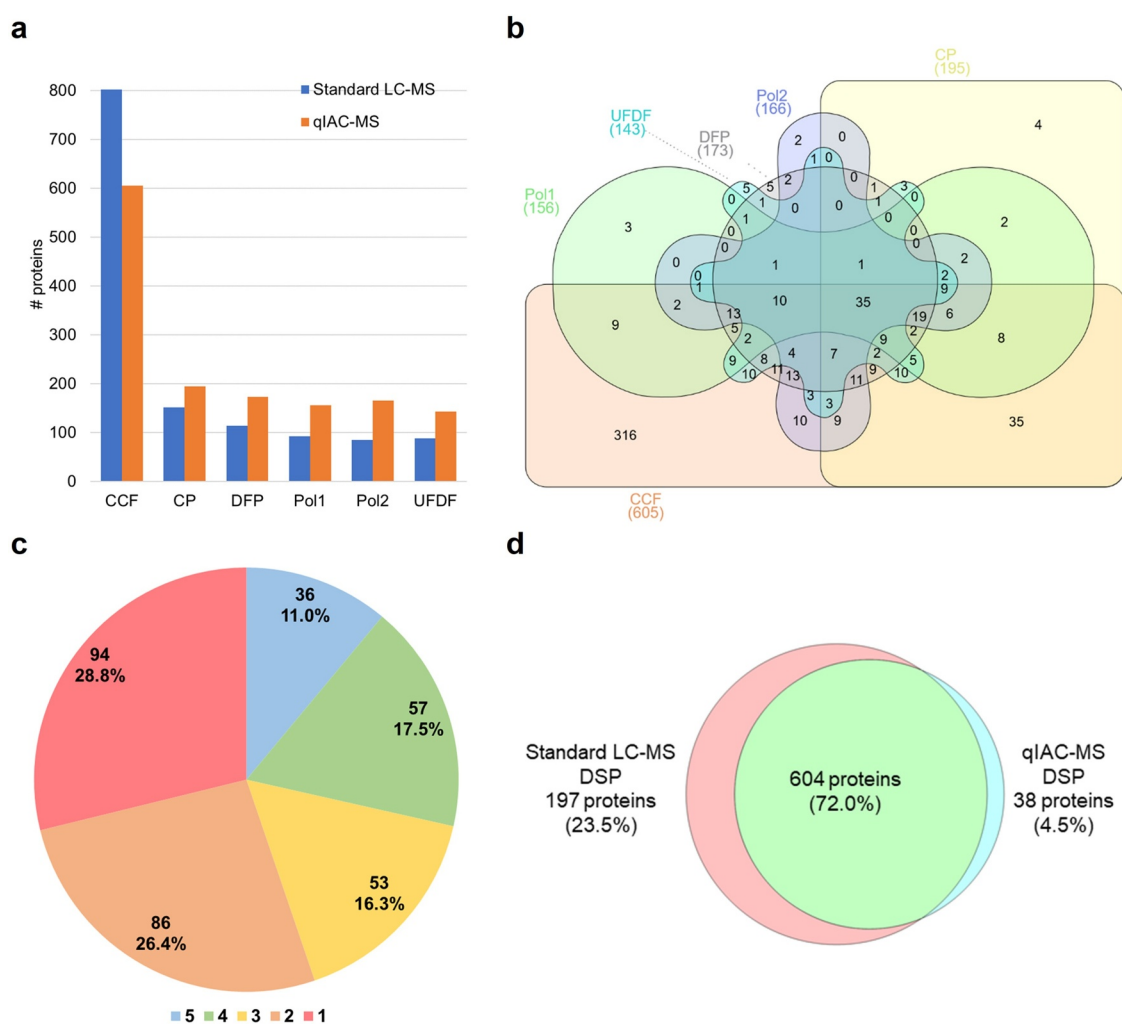


Figure 4. Comparison of DSP intermediates between standard LC-MS and qIAC-MS approach. (a) Number of identified HCPs in DSP intermediates by standard LC-MS (blue) and qIAC-MS (orange). (b) Venn diagram of HCPs identified by qIAC-MS approach within the different DSP intermediates: product cell culture fluid (Product CCF, orange), capture pool (CP, yellow), depth filter pool (DFP, gray), polishing 1 (Pol1, green), polishing 2 (Pol2, purple), and ultrafiltration/diafiltration (UFDF, cyan). The majority of HCPs were uniquely identified in Product CCF. A total of 35 HCPs were commonly identified in all six intermediates. (c) Pie chart of HCPs identified by qIAC-MS in DSP intermediates (except Product CCF). HCPs were identified in at least one (red), two (orange), three (yellow), four (green) or all five samples (blue). (d) Venn diagram of HCPs identified by standard LC-MS analysis compared to qIAC-MS approach of the complete DSP. The majority of HCPs (604 HCPs, 72.0%) were identified in LC-MS and qIAC-MS (green), whereas 197 HCPs (23.5%) were uniquely identified in LC-MS analysis (red) and 38 HCPs (4.5%) in qIAC-MS approach (cyan).

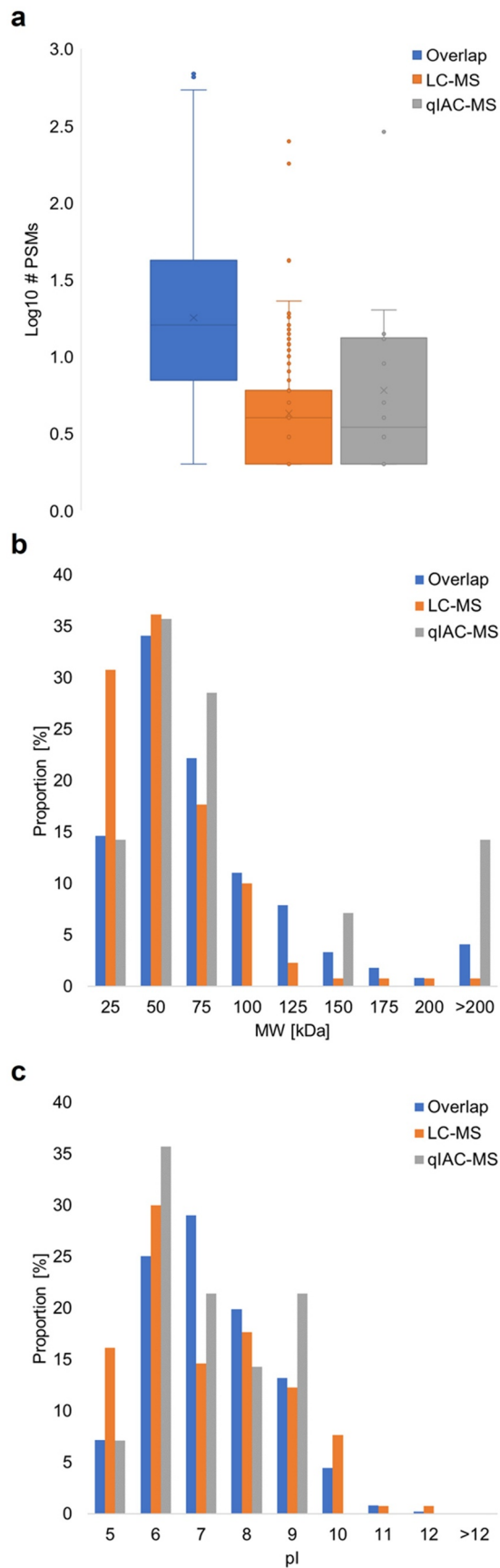


Figure 5. Characterization of the abundance (spectral counts) and physicochemical properties (MW and pI) of IAC-enriched and non-enriched HCPs of Mock CCF, Product CCF and DSP intermediates. (a) Box-plot of \log_{10} #PSMs (spectral counting by peptide spectrum matches) of HCPs identified in the overlap or uniquely in standard LC-MS or qIAC-MS approach. (b,c) Evaluation of the molecular weight (b) and pI (c) distribution of HCPs identified in LC-MS and qIAC-MS analysis (blue), uniquely identified in LC-MS (orange) or in qIAC-MS (gray) analysis.

HCPs enriched and detected solely after qIAC-MS were counted as positive for coverage determination.

Using the different calculation approaches, the following anti-HCP-Ab coverage values were achieved: 85.9%–84.8% (Mock CCF), 72.5%–64.8% (Product CCF), 74.8%–26.0% (CP), 76.9%–35.7% (DFP), 75.7%–28.6% (Pol1), 79.0%–22.9% (Pol2), 76.1%–23.3% (UFDF) (Table 2 and Figure 6). For Mock and Product CCFs only minor differences were observed when applying the different calculation approaches for coverage determination (overlapping or total qIAC-MS HCPs), whereas the DSP intermediates were substantially affected by the stringency level. In the latter, use of the overlapping HCPs from standard LC-MS and qIAC-MS analysis had a significant impact on the coverage calculation. Here, the determined coverage was reduced by a maximum of 40.1% (Pol2 intermediate, fivefold stringency). The influence of the different levels of stringency had a minor impact on the coverage calculation of the DSP intermediates and a negligible impact on the Mock and Product CCFs calculation. Nevertheless, the coverage determination using the qIAC-MS approach revealed high,

but not complete coverage by the ELISA antibody for Mock and Product CCFs, as well as for the complete DSP.

Coverage analysis with application of gel-based approach

The current standard for determination of ELISA antibody coverage is gel-based approaches, such as 2D-Western blot or 2D-DIGE. Here, we applied 2D-PAGE/2D-Western blot coverage analysis of Mock fermentation to allow direct comparisons with MS data.

A total of 564 and 535 spots were detected by silver stained 2D-PAGE and 2D-Western blot of CCF from Mock fermentation, respectively (Figure 7a). However, the intersection of the spot patterns between silver stained 2D-PAGE and 2D-Western blot was small. Overall, silver stain and Western blot overlapped at only 348 spots (46.3%), whereas 216 spots (28.8%) were uniquely detected in silver stained 2D-PAGE, and 187 spots (24.9%) uniquely detected in 2D-Western blot of Mock fermentation (Figure 7b). This resulted in an anti-HCP-Ab coverage of 61.7% (348 overlapping spots divided by all 564 spots detected in silver stained 2D-PAGE).

As the detection of spots in 2D-Western blot showed an MW dependency, we investigated the higher and lower MW ranges separately. The overlay of silver stained 2D-PAGE and 2D-Western blot showed a good match among high-abundance spots in the higher MW range (above ~25 kDa). Here, an intersection of 49.4% (256 spots) and a coverage of 65.3% was determined (256 overlapping spots divided by 392 spots detected in silver stained 2D-PAGE above ~25 kDa) (Figure 7c). However, in the lower MW range (<25 kDa) and the basic area only a few spots were detected in the immunoblot, whereas in the silver stained 2D-PAGE high-abundance spots were detected. Here, an intersection of only 39.5% (92 spots) and a coverage of 53.5% was achieved (92 overlapping spots divided by 172 spots detected in silver stained 2D-PAGE above <25 kDa) (Figure 7d). The ELISA antibody coverage for Mock fermentation determined by the gel-based approach was substantially lower compared to the qIAC-MS approach. Moreover, the gel-based approach revealed clear differences between spot patterns of the 2D-PAGE and the anti-HCP-Ab immunoblot.

Table 2. Results of ELISA antibody coverage determination of Mock fermentation (Mock CCF), product cell culture fluid (Product CCF), and DSP intermediates (capture pool (CP), depth filter pool (DFP), polishing 1 (Pol1), polishing 2 (Pol2), ultrafiltration/diafiltration (UFDF)). The preferred approach for ELISA antibody coverage determination (1.5-fold, total) is marked with an asterisk.

Sample	Anti-HCP-Ab Coverage [%] (1-fold)		Anti-HCP-Ab Coverage [%] (1.5-fold)		Anti-HCP-Ab Coverage [%] (2-fold)		Anti-HCP-Ab Coverage [%] (5-fold)	
	Overlap	Total	Overlap	Total*	Overlap	Total	Overlap	Total
Mock CCF	85.5	85.9	85.3	85.7	85.2	85.6	84.8	85.1
Product CCF	71.3	72.5	70.0	71.3	69.6	70.9	64.8	66.1
CP	56.7	74.8	45.3	65.3	40.0	61.0	26.0	49.5
DFP	53.6	76.9	47.3	72.2	43.8	69.9	35.7	64.0
Pol1	45.1	75.7	38.5	71.4	33.0	67.4	28.6	63.1
Pol2	47.0	79.0	42.2	75.8	34.9	71.7	22.9	63.0
UFDF	47.7	76.1	34.9	67.8	31.4	65.1	23.3	58.8

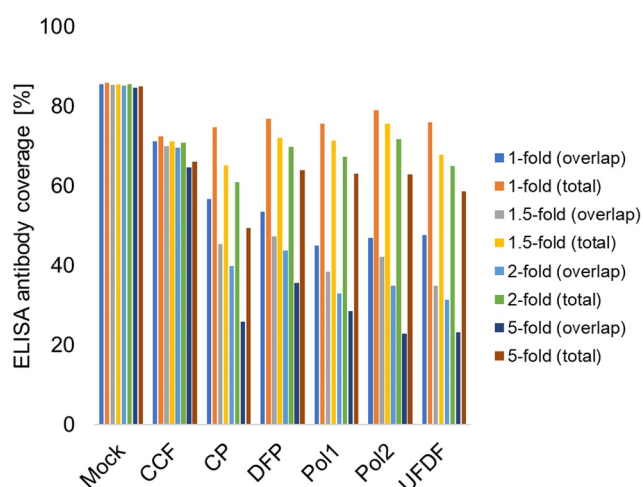


Figure 6. Results of ELISA antibody coverage determination. Shown are the different process samples (Mock fermentation (Mock CCF), product cell culture fluid (Product CCF), capture pool (CP), depth filter pool (DFP), polishing 1 (Pol1), polishing 2 (Pol2), ultrafiltration/diafiltration (UFDF)) with the associated levels of stringency (1-fold, 1.5-fold, 2-fold, 5-fold) and the different calculation approaches (Overlap or Total).

Discussion

HCP pattern of immunogen and Product CCF

For generating polyclonal antibodies used in the anti-HCP ELISA for mammalian cells, HCP material usually is taken from a mock fermentation to cover the broadest possible spectrum of HCP contamination. However, by introduction of the drug product into the cell line, the HCP pattern may be altered either quantitatively or by expression of different HCPs. Although it has been shown in different publications that the effect on different HCP species is “more similar than different” when comparing different transfected cell lines for production of biopharmaceuticals,^{23,33,34} meaningful differences may remain between individual manufacturing processes. As such, a detailed characterization by quantitative proteomics would substantially improve the understanding of a specific bioprocess. Therefore, we first evaluated the consistency between

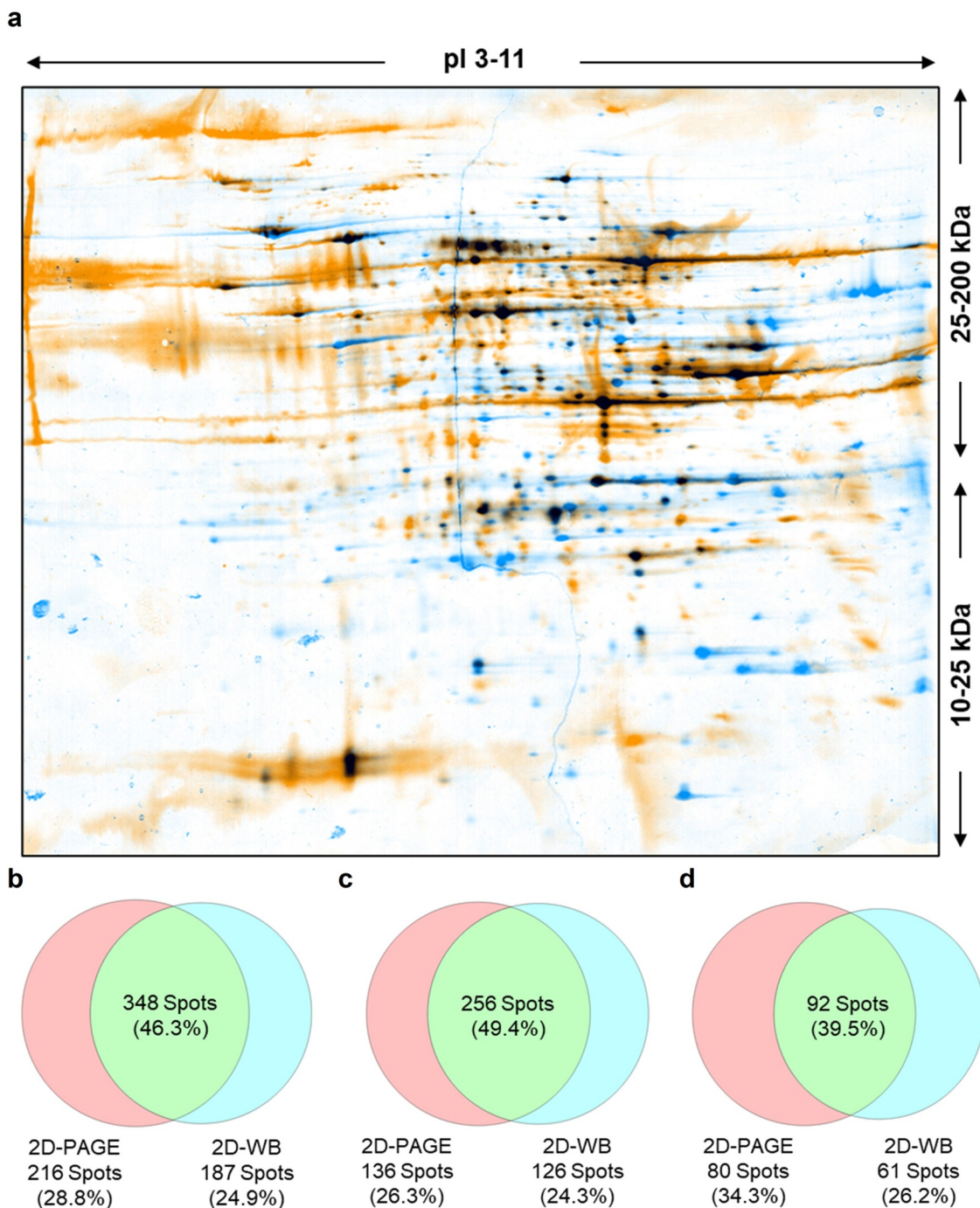


Figure 7. Results of 2D-Western blot analysis. (a) Overlaid images of silver stained 2D-PAGE (blue) and immunodetected 2D-Western blot (orange) of Mock fermentation (Mock CCF). Matched protein spots appear black. (b) Venn diagram of silver stained 2D-PAGE compared to 2D-Western blot. Most of the spots (348, 46.3%) were detected in the intersection of 2D-PAGE and 2D-Western blot (green), whereas 216 spots (28.8%) were uniquely detected in 2D-PAGE (red) and 187 spots (24.9%) in 2D-Western blot (cyan). (c,d) Venn diagrams of detected spots within the MW range of 25–200 kDa (c) and 10–25 kDa (d).

Mock and Product CCFs by standard LC-MS. The total number of identified proteins within the CCFs is in agreement with current studies examining the CHO proteome or secretome.^{19,33,34} As anticipated from previous study, HCP expression between both materials was observed to be highly similar.²³ Most of the HCPs exhibited a comparable abundance between Mock and Product CCF, but we found that some basic proteins or proteins with a lower MW are overrepresented, but not uniquely identified, in Product CCF. The unique HCPs identified either in Mock CCF or in Product CCF were all at

low abundance, indicating a potential shift of the dynamic range of the LC-MS assay for determining HCP abundance in the drug product or in the fermentation process. In some cases, a mock fermentation is performed to mimic a scenario with enhanced HCP levels. In the mock fermentation used for this investigation, the fermentation time was prolonged for approximately 24 hours to enhance the HCP levels in Mock CCF. However, the unique HCPs corresponded to the distribution of the common HCPs, leading to the conclusion that no protein groups were unique to either material with respect to

MW or pI. Therefore, it can be concluded that CCF of the mock fermentation represents most HCPs that are relevant for related bioprocesses, even if the conditions of the fermentations are changed toward more stress for the cells. This result thus strengthens the previous findings that the same Mock CCF material is suitable for developing an anti-HCP ELISA as platform method for different drug products and different processes. Furthermore, our data support the usage of Mock CCF as HCP Standard and antibodies obtained by immunization of Mock CCF are suitable for multi-product HCP ELISA. With respect to these results and regard to broader experience with product filings, it will be valuable to confirm the process-specific performance of the anti-HCP ELISA by determination of the antibody coverage in Product CCF once the commercial upstream production process is fixed.

IAC of HCP immunogen and DSP

IAC is a valuable tool for the enrichment of proteins and for the identification of protein–protein interactions.^{26,27} The IAC-MS combines the strengths of both techniques, i.e., the selective antigen–antibody interaction and the sensitivity of MS.^{28,29} The approaches described in the literature require biotinylation of the anti-HCP-Ab for coupling with subsequent purification and control of aggregation. Moreover, the quantification strategies used do not allow mapping of identifications between the different samples. This is particularly necessary, since the mass spectrometric analysis using the data-dependent acquisition approach favors high-abundance peptides for identification and prevents the measurement of low-abundance peptides.³⁵ Thus, HCPs with a lower abundance cannot be clearly determined as specifically or nonspecifically bound, if they are identified in only one sample. Our qIAC-MS approach has two advantages: (1) the anti-HCP-Ab directly can be used without prior biotinylation, and (2) the label-free quantification strategy enables the determination of specifically and nonspecifically bound HCPs, since identifications are mapped between the samples, especially lower abundant HCPs. However, IAC for ELISA antibody coverage determination can be challenging, due to usage of polyclonal antibody pools (anti-HCP-Ab) and complex and heterogeneous immunogens. Typically, very high product titers compared to low levels of HCPs is the main challenge for samples obtained during the DSP and the final product, and solutions to this problem, like peptide fractionation or native digestion of the HCPs without denaturation of the drug product, have been published.^{36–38} Furthermore, antigen-binding affinities and immunogenic HCP concentrations, limitation of anti-HCP antibody species and nonspecific binding to the IAC materials (e.g., column or beads), must be considered. Therefore, a suitable control strategy for nonspecific HCP binding is indispensable. The two different controls (BC and NC) used in our approach allowed the identification of HCPs already present in the anti-HCP-Ab (target contaminants) and those nonspecifically bound to the IAC material, and HCPs in both controls were evaluated quantitatively. For both controls, Mock and Product CCF, demonstrated high consistency between standard LC-MS and qIAC-MS analyses. The vast majority of HCPs were bound by the anti-HCP-Ab, with only minor alterations in the

abundance of each HCP. This suggests that an equilibration of the quantification is achieved by depletion of high abundance and enrichment of low abundance HCPs by IAC. However, different levels of individual HCPs were observed between qIAC-MS of Mock CCF compared to Product CCF. Here, the overlap between LC-MS and qIAC-MS for Mock CCF was higher than for Product CCF. A possible explanation could be the different dynamic ranges of the assays for HCP abundance in the materials. The high abundance of the API in Product CCF led to a decrease of overall HCP concentration, which results in a decreased identification rate by MS and technically lowering the HCP LC-MS signal below the detection limit.

In contrast to the complex Product CCF, the later DSP stages yield a different profile. Here, the samples showed an enrichment of individual HCPs by IAC compared to non-enriched CCF samples. Presumably, the lower complexity of process-related impurities in the DSP samples led to better isolation and identification of low-abundance HCPs by qIAC-MS. Considering the complete DSP, a similar HCP pattern was observed for LC-MS and qIAC-MS (72% overlapping HCPs), although 197 HCPs (23.5%) were not detected by the qIAC-MS approach. However, the major proportion of these HCPs (128 HCPs) is recognized by anti-HCP-Ab in Mock CCF. This indicates a technical challenge for the IAC method, rather than a detection gap of the anti-HCP-Ab.

ELISA antibody coverage determination by qIAC-MS

For determination of ELISA antibody coverage, a quantitative label-free proteomics approach was applied. Two different controls were used to identify and remove nonspecific binders: (1) a bead control (BC; coupled anti-HCP-Ab without added antigen) and (2) a negative control (NC: antigen without coupled anti-HCP-Ab). The 10 HCPs identified at low levels in the BC (mainly contaminants from sample preparation) were removed and not considered for further analysis. The NC for each CCF sample was compared quantitatively to the corresponding IAC data. The applied label-free quantification approach enables the mapping of identifications between IAC and NC and the determination of specifically and nonspecifically bound HCPs, even those with low abundance. To account for the variability of the applied label-free quantification approach (20%–50%),^{30–32} the data were parsed into four different stringency levels for the consideration of the negative control to assess and establish a suitable criterion. The stringency levels (fold change IAC to NC) consider different variabilities of the HCP quantification: (a) 1-fold (no variability considered), (b) 1.5-fold (50% variability considered), (c) 2-fold (100% variability considered), or (d) 5-fold (500% variability considered). This means that a difference in abundance of 1-fold does not take variability into account and thus yields low confidence in the determination of specifically and nonspecifically bound HCPs, whereas a difference of 5-fold provides a high confidence determination.

The different levels of stringency had only a marginal effect on the coverage for Mock and Product CCF. The Mock showed the highest coverage of the ELISA antibody (~85%), whereas for Product CCF (~70%) the coverage was lower. The lower

coverage in Product CCF can be explained by the presence of the highly abundant API. So, the given matrix may have an impact on the dynamic range of HCP concentration determination, as described above in the section on IAC of CCF and DSP samples. For the DSP intermediates, a minor effect on the coverage at different levels of stringency was observed, indicating a higher degree of nonspecific binding in these samples. The nonspecific binding to the bead material predominated over the specific binding to the anti-HCP-Ab due to the very low abundance of HCPs within the DSP intermediates. This leads to an equalization of the HCP abundances between the NC and the IAC, and thus to a decreased anti-HCP-Ab coverage when considering the NC quantitatively. As such, the usage of negative controls is indispensable for a reliable and confident determination of ELISA antibody coverage specificity and to support comparison of data between products and between independent assays. Based on recent literature, the variability of the label-free approach has been reported in the range of 20%–50%,^{30–32} therefore, it follows that a suitable stringency threshold (fold change IAC to NC) for the quantitative consideration of the NC is 1.5-fold (corresponds to 50% variability). The analysis of stringency levels here shows that both 1.5-fold and a stricter threshold of more than 2-fold may also be used without changing the coverage results.

Different approaches to the coverage calculation were investigated, either using only the HCPs identified at the overlap of standard LC-MS and qIAC-MS or the total number of HCPs identified in qIAC-MS. From the experiments performed within this study, it can be assumed that this factor only has marginal influence on complex samples (Mock and Product CCF), but a substantial impact on the partly purified and less complex DSP intermediates. Here, the determined coverage was almost 50% lower when using only the overlapping HCPs instead of including the HCPs solely identified in the DSP samples. An explanation for this could be that there are different dynamic ranges for the determination of HCP concentration between the two methods. In the standard LC-MS approach, the high abundance of the API and/or other process-related impurities superimposes on the low-abundance HCPs, whereas when applying IAC, the HCPs are substantially enriched and the API depleted. The latter results in a better HCP isolation by antibody binding and enhanced identification of low-abundance HCPs. Overall, this leads to a higher identification rate in the IAC-enriched samples and a lower one in the non-enriched samples. Using negative controls for quantitative determination and the resulting identification of nonspecific binders, the total number of HCPs identified by qIAC-MS for coverage determination is improved, likely because these proteins must be from the specific sample but may be in too low abundance for detection without IAC-enrichment. For this reason, it can be suggested that using the total number of HCPs identified in qIAC-MS is a suitable approach for calculation of the anti-HCP-Ab coverage.

Assessment of ELISA antibody coverage

Using the qIAC-MS approach, we confirmed that high ELISA antibody coverage was achieved with the anti-HCP-Ab reagent. Approximately 13% of HCPs (130 of 963 HCPs)

identified by standard LC-MS were not found to be covered by the anti-HCP-Ab ELISA antibody. One possible reason for this may be the low abundance of these HCPs in the immunogen so that no or low antibody titer of mainly low-affinity antibodies were developed in the animal. In combination with experimental conditions, this may further lead to antibodies by loss, e.g., during the washing steps.

As expected, based on previous findings,²³ the anti-HCP-Ab coverage, considering the complete bioprocess, was similar as for the CCF of the mock fermentation. This indicates that use of the Mock CCF for coverage analysis is relevant, as the majority of HCPs are covered by the anti-HCP-Ab for the complete bioprocess. Although the determination of antibody coverage by IAC has significant advantages compared to the 2D-Western blot method, IAC still has limitations in the presence of high levels of drug product. Again, the results from Mock CCF anti-HCP-Ab coverage can answer the question if the absence of coverage for individual HCPs is caused by a lack of specific antibodies (HCP not detected in Mock CCF) or a technical limitation due to high product concentration (HCP detected in Mock CCF). In such cases, the true value of anti-HCP-Ab coverage is underestimated.

Overall, the qIAC-MS approach presented here is suitable for ELISA antibody coverage determination and allows the identification of covered and non-covered HCPs, improving risk assessment for analytical quality and patient safety. The knowledge of the presence or absence of ELISA antibodies that bind specific HCPs in the Mock CCF is highly relevant to the quality of the given antibody reagent coverage. In case this HCP species would occur with increased levels of the drug substance, this will most probably result in a higher ELISA value given by the immunological weighted ELISA result and ensured by the serial dilutions in a suitable HCP ELISA plate layout. Therefore, the knowledge of each HCP species not detected by the ELISA antibodies can be the basis for increasing the quality of the HCP analysis by, for example, additional testing of individual “high risk” HCPs with potential to affect product stability and quality and patient safety in a case-specific manner.

Comparison of qIAC-MS with gel-based approach

Gel-based approaches like 2D-Western blot analysis are well-established standard methods for ELISA antibody coverage determination.¹² Here, the spot pattern of a silver stained 2D-PAGE of a Mock CCF was compared to a 2D-Western blot with the anti-HCP-Ab as primary antibody. 2D gel analysis approaches have some limitations, such as potentially incomplete HCP resolution or complex spot patterns due to extensive HCP and product modifications, such as post-translational modifications. Moreover, the coverage determination relies mostly on visual comparison and no simultaneous identification of HCPs is possible. As it is widely accepted by the industry and regulators that gel-based approaches are still a usable standard for determination of antibody coverage, a comparison of this qIAC-MS approach with the current standard has substantial value.

Anti-HCP-Ab coverage data derived from 2D-Western blot analysis were compared with the qIAC-MS of Mock CCF. The ELISA antibody coverage for Mock CCF determined by the

qIAC-MS approach (~86%) was significantly higher than the gel-based approach (~62%). Furthermore, the absolute number of HCPs considered for coverage determination was higher for qIAC-MS (956 HCPs) than for the gel-based approach (751 spots). Spots in the gel-based approach may include an unknown number of identical HCP species with different modifications, which must also be taken into account. In this study, the gel-based approach revealed clear differences between the spot patterns of the 2D-PAGE and anti-HCP-Ab immunoblot. The low overlap of spots in 2D-PAGE and 2D-Western blot is partially caused by spots detected solely by the sensitive immunoblot compared to the silver stain and reveals a technical limitation of the 2D-PAGE analysis. However, in the 2D-PAGE as well as in the qIAC-MS approach, HCPs with an MW below 25 kDa or in the basic region (around pI 9) were substantially underrepresented in this analysis, which is in agreement with recent literature.²⁸ Based on broader experience with different HCP ELISA antibody productions, it seems likely this may be due to a lower immune response against some HCPs with low MW. On the one hand, the number of epitopes is limited to small proteins, and, therefore, the ability to induce an antibody response in the animal by an immunogenic epitope is reduced statistically compared to a large protein with multiple epitopes. On the other hand, it can be speculated that small proteins with basic or acidic PI are more prone to denaturation or even not soluble under the neutral buffered pH conditions of the HCP suspension used for injection or the conditions after injection of the HCPs into the animal's skin. Therefore, the limited number of epitopes suitable to induce antibody production against the native HCP may be further reduced by denaturation, especially for HCPs with acidic and basic pI. Overall, the qIAC-MS approach overcomes some limitations of the 2D-Gel approaches, but still the complex matrix of CCF and the low levels of HCPs poses a challenge in HCP analysis for both described methods.

In conclusion, a well-characterized HCP ELISA showing process-related performance by detecting a broad range of HCPs is the current analytical gold standard for biopharmaceutical batch release testing of commercial biopharmaceutical products. From the presented data, it is clear our qIAC-MS approach is suitable for ELISA antibody coverage determination and allows for the identification of covered and non-covered HCPs by the ELISA, leading to an improvement in risk assessment of HCP content in biopharmaceutical products. The combination of highly specific antigen-antibody interactions in IAC and the sensitivity of MS-based protein detection enables good coverage determination across a broad range of HCPs with respect to MW and pI. The virtual 2D visualization of the identified HCPs presents results in a visual way akin to 2D-Gel analysis or the data can be presented in a list that includes data quality parameters for identified HCPs. The generated list of HCPs may be further used for database implementation and digitalization for more sophisticated analyses over different products, processes and/or timepoints of testing to gain generalizable HCP knowledge over time.

The method presented here allows label-free identification and relative quantification of HCPs that exhibit immunoreactivity even at very low abundance in the sample. To our knowledge, for the first time, the approach was shown here to be

applicable for the analysis of process samples containing high-abundance API. Compared to 2D-PAGE and 2D-Western blot, which is the current standard for determination of HCP coverage for anti-HCP antibodies in biopharmaceutical quality control, this method: (1) typically detects more HCP species; (2) allows the identification of the detected HCP species; (3) allows relative quantification of individual HCPs even in the presence of highly abundant API; and (4) assays the antibody binding under conditions more comparable to the ELISA testing than the denaturing conditions of a 2D-Western blot. Besides the substantial benefits of the qIAC-MS approach presented herein, some limitations were identified. First, there is a need for suitable controls for each run of the IAC workflow due to the high sensitivity of the LC-MS detection. Nonspecific HCP binding to material and equipment can be reduced but not completely avoided, so a threshold approach for specific enrichment by IAC should be utilized. Second, only if the quantitative IAC performs highly reproducibly for different analytical runs, than it is possible to compare the results obtained on different days or among different products. Finally, expert knowledge about the evaluation of complex MS data is required. Nonetheless, once the qIAC-MS approach is established, it provides a detailed picture of the ELISA antibody binding and possible detection gaps of the ELISA, and it also enables a significant improvement in risk assessment and mitigation by identification the HCP species present and enrichment of low abundance species during DSP. This is essential for HCP detection gap risk mitigation. For example, comparing direct HCPs and IAC HCP detection from samples with high HCP levels (CCF) can be used as the basis for identification of possible HCP detection gaps of the ELISA antibody with a particular focus on already described high-risk HCPs.²⁵ The relevance of these gaps can be further assessed for correlation in samples like UFDF or DS for different bioproducts.

Overall, this study demonstrates that combining IAC with MS detection applies quantitative proteomics for HCP characterization and improves the quality of the characterization of the anti-HCP-Ab compared to 2D-Western blot analysis for antibody coverage determination. The approach has proven valuable to our product and process development and is being implemented broadly across biological programs for assessing HCP ELISA coverage, which is an important criteria for HCP assay quality. Furthermore, our data show that it is a powerful tool to enrich those HCPs that are detected by the antibodies in samples with low and very low HCP abundance. We believe broad implementation of the approach will further increase knowledge about whether individual residual HCPs in biopharmaceuticals may affect product efficacy or stability, leading to improved efficiency in product purification process and improved knowledge of the purity of biopharmaceutical products.

Materials and methods

Cell lines and bioreactor cultures

The cell lines used for Mock and for product production used here originate from CHO cells isolated by Tjio and Puck.³⁹

Both cell lines belong to the subpopulation of CHO DUKX (CHO DG-44) cells. These cells were generated by mutagenizing the CHO subclone to create a missense mutation in one allele and a deletion in the other allele of the dihydrofolate reductase gene.⁴⁰ Both cell lines were adapted to suspension growth and only the production cell line was stably transfected to express a mAb IgG1. For production of HCPs from both mock and product, frozen cell stocks were maintained in cell banks, thawed and scaled up in shake flasks, small-scale bioreactors and mid-size bioreactors. Bioreactor conditions are related to the Boehringer Ingelheim proprietary platform process, and cultivation of the product was in 12000 L scale. The Mock process varies from the mAb product process in that it has a 24 h elongated process time before harvest to increase HCP levels. The Mock transfected cell line does not express a product and was cultivated in a 200 L stirred tank. The following product process samples were tested: Product cell culture fluid (Product CCF) contains filtered, cell free supernatant at the end of fermentation; downstream process intermediates (capture pool (CP); depth filter pool (DFP); and anion exchange and cation exchange chromatography polishing 1 (Pol1) and polishing 2 (Pol2)). The DSP sample ultrafiltration/diafiltration (UFDF) is the last process step before formulation of Drug Substance.

Generation of anti-HCP-Ab

The anti-HCP-Ab was derived by a 200 L fermentation, with a cell line lacking the coding sequence for the mAb IgG1 API. The fermentation parameters for this “Mock” fermentation were closely related to the proprietary Boehringer Ingelheim platform process with the exception that the fermentation time was extended for 2 d. This extension increased the level of HCPs in the cell-free culture supernatant at the end of fermentation. Immunization with the cell-free supernatant at the end of fermentation was performed in rabbits. A fraction of the rabbits were immunized with the total HCP content, and the second fraction was immunized using a low MW fraction of the HCPs to enhance antibody levels against low MW HCPs. The different antibody sera were purified by anti-HCP immunochromatography against their respective HCP fraction. Finally, the purified HCP fractions were pooled so that detection of low MW HCPs detection was improved compared to the total HCP antibody fraction alone.

Two-dimensional gel electrophoresis

Buffer components were added to the sample to a final concentration as follows: 1% CHAPS, 70 mM dithiothreitol (DTT), 7 M urea, and 2 M thiourea. The sample was concentrated using Amicon Ultra Ultrafiltration Units (3 kDa cutoff). The protein amount of the sample prior to 2D gel electrophoresis was determined using an established method according to Popov et al.⁴¹ IEF was performed as described elsewhere.⁴² Briefly, 20 cm gels containing 9 M urea, 3.5% acrylamide, 0.3% piperazine diacrylamide, and a total of 4% carrier ampholyte pH 2–4 were used. The samples were applied onto the IEF gels on the anodic side of the tube gels. The proteins were focused under nonequilibrium pH gradient electrophoresis

conditions (NEPHGE) for 21 h and 15 min. The IEF gels were applied onto SDS gels of 0.75 × 250 × 300 mm³ containing 15% acrylamide and 0.2% bis-acrylamide using the IEF gels as stacking gels. The proteins were separated according to their apparent MW in a continuous buffer system (25 mM Tris, 192 mM glycine, and 0.1% SDS). The separated proteins were visualized with silver stain to achieve the highest sensitivity.

Two-dimensional Western blot and immunodetection

For Western blotting, the 2D gel was continuously blotted using a semi-dry electro blot (0.8 mA/cm²) with a transfer buffer containing 50 mM Tris base, 300 mM glycine, 10% methanol, and 0.25% SDS onto PVDF membrane. After blocking with Roti-Block for 2 hours, the blot was incubated with anti-HCP-Ab in block buffer with a concentration of 10 µg/mL overnight at 5°C. The blot was incubated with the secondary antibody anti-rabbit IgG HRP-conjugated (1:2000) in block buffer for at least 1.5 h. The blot was developed using 3,3'-diaminobenzidine substrate.

Data evaluation 2D-PAGE and 2D-Western blot

The digitized images were compared using Decodon Delta2D 4.8.0. Every detected spot was checked manually. Spots in the silver-stained gel and the immunodetected Western blot were counted. The number of digitally detected spots was compared to the manually counted spots in the silver-stained gel. Both images were overlaid, and the immunodetected Western blot spots were assigned to the spots of the silver staining to identify detection gaps. To calculate an overlap of detected spots resulting from silver staining and immunodetection, a “fused” image of silver staining and Western blot was generated. This fused image then was compared with the individual silver-stained gel and Western blot image for identification of differences in the spot patterns between the two detection methods.

Immunoaffinity chromatography

For IAC, epoxy magnetic beads were used to generate two types of bead materials, and IAC was performed using Dynabeads® M-270 Epoxy (Thermo Fisher Scientific). The magnetic spheres contain epoxy groups as functional groups that react with primary amines of proteins or other molecules and form stable amide bonds. To remove interfering buffer components, the anti-HCP-Ab was rebuffed by ultrafiltration against 50 mM borate buffer, pH 8.5 using an Amicon Centrifugal Filter Unit with Ultracel-50 membrane (Merck Millipore), according to the manufacturer's instructions. The protein concentration was determined by UV measurement (absorption at 280 nm).

For antibody coupling to generate the coupled bead material for the Bead Control (BC) and IAC, the magnetic beads were incubated along with the anti-HCP-Ab overnight at 37°C. Subsequently, unbound antibody was removed in different wash steps. To inhibit any further coupling reactions at unreacted sites, the magnetic beads were blocked for 2 h at ambient temperature using 5% bovine serum albumin (BSA). This bead material was then used for the Bead Control (BC;

anti-HCP-Ab coupled beads without exposure to CCF HCPs) and for IAC analysis (anti-HCP-Ab coupled beads with exposure to CCF HCPs). To generate the Negative Control (NC) bead material, magnetic beads without coupled antibody were prepared to define nonspecific binding. Here, the magnetic beads were incubated with 50 mM borate buffer overnight at 37°C and blocked with BSA as described above. For IAC and NC, both sets of magnetic beads were incubated with the HCPs of the respective process sample overnight at 37°C. Here, the NC was performed for each process sample (including the DSP samples). Unbound antigen was removed in different wash steps. HCPs bound to the antibody coupled IAC and NC bead materials were eluted using 0.1 M glycine pH 2 for 1 h at ambient temperature. For in-solution digestion, the pH of the eluate was adjusted to pH 8 using 1 M ammonium bicarbonate.

Sample preparation for MS analysis

For LC-MS analysis, the samples were initially concentrated and rebuffed. The samples were precipitated with 33% (w/v) trichloroacetic acid with a final concentration of 7% (w/v) for 45 min on ice. Subsequently, the samples were washed with acetone and resuspended in 8 M urea buffer. The protein concentration was determined by 660 nm Assay (Thermo Fisher Scientific) measurement according to the manufacturer's instructions. For further sample preparation, the samples were diluted with 50 mM ammonium bicarbonate to a final concentration of 1 M urea. The proteins were reduced to 10 mM DTT for 15 min at 60°C and alkylated using 30 mM iodoacetamide at ambient temperature for 30 min in the dark. The alkylation reaction was quenched by the addition of 100 mM DTT. Afterward, the proteins were proteolytically cleaved with trypsin (1:20) overnight at 37°C. The reaction was stopped by acidification with trifluoroacetic acid to a final concentration of 1%. The digested samples were concentrated to dryness using vacuum concentrator.

HPLC-MS/MS data acquisition

HPLC-ESI-MS and -MS/MS mass spectra were obtained using an UltiMate® 3000 RSLCnano System (Thermo Fisher Scientific) coupled to a Q Exactive HF-X Orbitrap mass spectrometer (Thermo Fisher Scientific). The separation of peptides was performed with reversed-phase (RP) chromatography. Separator column Acclaim PepMap RSLC C18 column (300 μ m I.D. \times 150 mm, 2 μ m particle size, 100 Å pore size, Thermo Fisher Scientific) was used. Eluents were A: water/0.1% formic acid; B: acetonitrile/0.1% formic acid. The peptides were separated using a segmented gradient from 2% B to 50% B in 91 min at 40°C with a flow rate of 5 μ L/min. MS and MS/MS spectra were recorded in positive ion mode with internal mass calibration. MS/MS spectra were produced with higher-energy collisional dissociation applying a normalized collision energy of 28. A TOP10-data-dependent acquisition with polysiloxanes as lock masses and dynamic exclusion of already measured ions was applied. Additional blank runs were performed to identify carryover proteins.

Identification and quantification of proteins

For unbiased identification and label-free quantification of proteins, the MS data sets were analyzed with Proteome Discoverer 2.2 (Thermo Fisher Scientific).

Protein identification was achieved by database searching using MS Amanda 2.0 (as implemented in Proteome Discoverer). The mass spectra were matched against a database consisting of a list of common contaminants from sample preparation, the sequences of the API (light and heavy chain) and a NCBI-CHO database (generated on 05.08.2020, taxonomy: *Cricetulus griseus* (tax ID 10029), 94975 entries). The search parameters were used as following: enzyme: trypsin (full), maximum missed cleavages: 2, taxonomy: all, MS tolerance 10 ppm, MS/MS tolerance 10 ppm, static modification: Carbamidomethyl (C), dynamic modifications: Oxidation (M), Deamidation (NQ), and Acetylation (peptide N-term). For False Discovery Rate (FDR) calculation, we applied a decoy approach based on reversed protein sequences. The peptide identification was based on an FDR below 0.05, on peptide spectrum match (PSM), and protein level. Protein grouping was performed. In case of ambiguous protein identification, only one isoform of a protein is reported. A minimum of 2 unique peptides over all datasets were required for identification. Unique peptides are peptides which are unique to the sequences of the specific protein group. Contaminants were removed for further analysis.

For quantification, a label-free approach was applied. Here, the corresponding MS signal of high confidence (1% FDR) identified peptides was matched to all data sets based on a tolerance of 10 ppm and a retention time window of 4 minutes. This enabled the detection of low abundance peptides in additional datasets. Proteins were quantified based on the intensity of at least two unique peptides of a protein. The samples were normalized to the total protein abundance (summed intensity of all identified proteins) of the respective samples.

Calculation of antibody coverage

Antibody coverage for anti-HCP-Ab determined by qIAC-MS approach was calculated by using label-free quantification. HCPs identified in standard LC-MS measurement of a sample were compared with the identified HCPs in the respective IAC sample. The anti-HCP-Ab coverage was calculated by excluding all HCPs that were identified within the Bead Control (contaminants in anti-HCP-Ab) and that show a higher or similar abundance in the Negative Control (nonspecific binding of HCPs to bead material) compared to the IAC antigen sample (antibody bound, nonspecifically bound, and contaminants from anti-HCP-Ab reagent, i.e., NC \geq IAC). Different levels of stringency (ratio IAC to NC, fold change) were applied as thresholds: HCPs that were (a) 1-fold, (b) 1.5-fold, (c) 2-fold, or (d) 5-fold lower abundance in the IAC analysis compared to the NC were not considered as enriched, and, therefore, were not used in the coverage determination at each threshold level. For calculation of the coverage, either the HCPs identified in the overlap of LC-MS and the qIAC-MS (overlap; overlapping HCPs divided by all HCPs detected in standard LC-MS) or the total number of HCPs identified in qIAC-MS (total; all HCPs detected in qIAC-MS divided by all HCPs

detected in standard LC-MS) was used. For this, the respective number of HCPs (either overlap or total) was divided by the number of HCPs identified by LC-MS.

Antibody coverage for anti-HCP-Ab determined by gel-based approach was calculated by visual comparison of silver stained 2D-PAGE and 2D-Western blot. Here, the overlapping spots between 2D-PAGE and 2D-Western blot (intersection) were divided by all spots detected in silver stained 2D-PAGE. The spots uniquely detected in the 2D-Western blot were not considered as covered.

Abbreviations

Acknowledgments

The authors thank Dr Jennifer S. Chadwick for review of the manuscript, Goeran Huebner for his fruitful input as MS Expert, and Kirsten Ciupke for excellent technical assistance.

Disclosure statement

No potential conflict of interest was reported by the author(s).

2D	Two-dimensional
API	Active pharmaceutical ingredient
BC	Bead control
BSA	Bovine serum albumin
CCF	Cell culture fluid
CHAPS	3-[(3-Cholamidopropyl)dimethylammonio]-1-propanesulfonate
CHO	Chinese Hamster Ovary
CP	Capture pool
cQA	Critical quality attribute
DAB	3,3'-diaminobenzidine
DFP	Depth filter pool
DS	Drug substance
DSP	Downstream process
DTT	Dithiothreitol
ELISA	Enzyme-linked Immunosorbent Assay
FDR	False discovery rate
HCD	Higher energy collisional dissociation
HCP	Host cell protein
HPLC	High-performance liquid chromatography
HRP	Horseshoe peroxidase
IAC	Immunoaffinity chromatography
IEF	Isoelectric focusing
LC	Liquid chromatography
mAb	Monoclonal antibody
MS	Mass spectrometry
MS/MS	Tandem mass spectrometry
MW	Molecular weight
NBE	New biological entities
NC	Negative control
NCE	Normalized collision energy
NEPHGE	Nonequilibrium pH gradient electrophoresis
PAGE	Polyacrylamide gel electrophoresis
pI	Isoelectric point
Pol1	Polishing 1
Pol2	Polishing 2
PSM	Peptide spectrum match
PVDF	Polyvinylidene fluoride
qIAC	Quantitative immunoaffinity chromatography
SDS	Sodium dodecyl sulfate
UFDF	Ultrafiltration/Diafiltration

Funding

This work was financially supported by BI Global Technology Management: pid-2020-fea-0003.

References

1. U.S. Pharmacopeia Monograph <1132> Residual host cell protein measurement in biopharmaceuticals. Second supplement to USP38-NF33, 2016.
2. Ph. Eur. 9.1, 4041 (04/2017) Pharmacopoeia E. 2. 6.34 Host cell protein assays. EUROPEAN PHARMACOPOEIA. 2017; 91: 4041–45.
3. Bailey-Kellogg C, Gutiérrez AH, Moise L, Terry F, Martin WD, Groot ASD. CHOPPI: a web tool for the analysis of immunogenicity risk from host cell proteins in CHO-based protein production. *Biotechnol Bioeng* PMID: 24888712. 2014;111(11):2170–82. doi:10.1002/bit.25286.
4. Beatson R, Sproviero D, Maher J, Wilkie S, Taylor-Papadimitriou J, Burchell JM. Transforming growth factor- β 1 is constitutively secreted by Chinese hamster ovary cells and is functional in human cells. *Biotechnol Bioeng* PMID: 21618471. 2011;108(11):2759–64. doi:10.1002/bit.23217.
5. Gao SX, Zhang Y, Stansberry-Perkins K, Buko A, Bai S, Nguyen V, Brader ML. Fragmentation of a highly purified monoclonal antibody attributed to residual CHO cell protease activity. *Biotechnol Bioeng* PMID: 21404269. 2011;108(4):977–82. doi:10.1002/bit.22982.
6. Bee JS, Machiesky LM, Peng L, Jusino KC, Dickson M, Gill J, Johnson D, Lin H-Y, Miller K, Heidbrink Thompson J, et al. Identification of an IgG CDR sequence contributing to co-purification of the host cell protease cathepsin D. *Biotechnol Prog*. 2017;33(1):140–45. PMID: 27798957. doi:10.1002/btpr.2397.
7. Robert F, Bierau H, Rossi M, Agugiaro D, Soranzo T, Broly H, Mitchell-Logean C. Degradation of an Fc-fusion recombinant protein by host cell proteases: identification of a CHO cathepsin D protease. *Biotechnol Bioeng* PMID: 19655395. 2009;104(6):1132–41. doi:10.1002/bit.22494.
8. Chiu J, Valente KN, Levy NE, Min L, Lenhoff AM, Lee KH. Knockout of a difficult-to-remove CHO host cell protein, lipoprotein lipase, for improved polysorbate stability in monoclonal antibody formulations. *Biotechnol Bioeng* PMID: 27943242. 2017;114(5):1006–15. doi:10.1002/bit.26237.
9. Dixit N, Salamat-Miller N, Salinas PA, Taylor KD, Basu SK. Residual host cell protein promotes polysorbate 20 degradation in a sulfatase drug product leading to free fatty acid particles. *J Pharm Sci* PMID: 27032893. 2016;105(5):1657–66. doi:10.1016/j.xphs.2016.02.029.
10. Zhu-Shimoni J, Yu C, Nishihara J, Wong RM, Gunawan F, Lin M, Krawitz D, Liu P, Sandoval W, Vanderlaan M. Host cell protein testing by ELISAs and the use of orthogonal methods. *Biotechnol Bioeng* PMID: 24995961. 2014;111(12):2367–79. doi:10.1002/bit.25327.
11. Champion K, Madden H, Dougherty J, Shacter E. Defining your product profile and maintaining control over it, Part 2: challenges of monitoring host cell protein impurities. *BioProcess Intl*. 2005;3:52–57.
12. Shahrokh Z, Schmalzing D, Rawat R, Sluzky V, Ho K, Engelbergs J, Bishop J, Friedl E, Meiklejohn B, Ritter N. Science, risks and regulations. Current perspectives on host cell protein analysis and control. *BioProcess Int*. 2016;14:40–51.
13. Kornecki M, Mestmäcker F, Zobel-Roos S, Heikaus de Figueiredo L, Schlüter H, Strube J. Host cell proteins in biologics manufacturing: the good, the bad, and the ugly. *Antibodies (Basel)*. 2017;6:PMID: 31548528. doi:10.3390/antib6030013.
14. Tscheliessnig AL, Konrath J, Bates R, Jungbauer A. Host cell protein analysis in therapeutic protein bioprocessing - methods and applications. *Biotechnol J* PMID: 23436780. 2013;8(6):655–70. doi:10.1002/biot.201200018.
15. Wang X, Hunter AK, Mozier NM. Host cell proteins in biologics development: identification, quantitation and risk assessment.

- Biotechnol Bioeng PMID: 19388135. 2009;103(3):446–58. doi:10.1002/bit.22304.
16. Chevalier F. Highlights on the capacities of “Gel-based” proteomics. *Proteome Sci* PMID: 20426826. 2010;8(1):23. doi:10.1186/1477-5956-8-23.
 17. Doneanu CE, Chen W. Analysis of host-cell proteins in biotherapeutic proteins by LC/MS approaches. *Methods Mol Biol* PMID: 24648086. 2014;1129:341–50. doi:10.1007/978-1-62703-977-2_25.
 18. Reisinger V, Toll H, Mayer RE, Visser J, Wolschin F. A mass spectrometry-based approach to host cell protein identification and its application in a comparability exercise. *Anal Biochem* PMID: 24949901. 2014;463:1–6. doi:10.1016/j.ab.2014.06.005.
 19. Zhang Q, Goetze AM, Cui H, Wylie J, Trimble S, Hewig A, Flynn GC. Comprehensive tracking of host cell proteins during monoclonal antibody purifications using mass spectrometry. *Mabs* PMID: 24518299. 2014;6(3):659–70. doi:10.4161/mabs.28120.
 20. Walker DE, Yang F, Carver J, Joe K, Michels DA, Yu XC. A modular and adaptive mass spectrometry-based platform for support of bioprocess development toward optimal host cell protein clearance. *MAbs* PMID: 28346045. 2017;9(4):654–63. doi:10.1080/19420862.2017.1303023.
 21. Zhang Q, Goetze AM, Cui H, Wylie J, Tillotson B, Hewig A, Hall MP, Flynn GC. Characterization of the co-elution of host cell proteins with monoclonal antibodies during protein A purification. *Biotechnol Prog* PMID: 27073178. 2016;32(3):708–17. doi:10.1002/btpr.2272.
 22. Kreimer S, Gao Y, Ray S, Jin M, Tan Z, Mussa NA, Tao L, Li Z, Ivanov AR, Karger BL. Host cell protein profiling by targeted and untargeted analysis of data independent acquisition mass spectrometry data with parallel reaction monitoring verification. *Anal Chem* PMID: 28402653. 2017;89(10):5294–302. doi:10.1021/acs.analchem.6b04892.
 23. Falkenberg H, Waldera-Lupa DM, Vanderlaan M, Schwab T, Krapfenbauer K, Studts JM, Flad T, Waerner T. Mass spectrometric evaluation of upstream and downstream process influences on host cell protein patterns in biopharmaceutical products. *Biotechnol Prog* PMID: 30767403. 2019;35(3):e2788. doi:10.1002/btpr.2788.
 24. Vanderlaan M, Zhu-Shimoni J, Lin S, Gunawan F, Waerner T, Van Cott KE. Experience with host cell protein impurities in biopharmaceuticals. *Biotechnol Prog* PMID: 29693803. 2018;34(4):828–37. doi:10.1002/btpr.2640.
 25. Jones M, Palackal N, Wang F, Gaza-Bulseco G, Hurkmans K, Zhao Y, Chitikila C, Clavier S, Liu S, Menesale E, et al. “HIGH-RISK” HOST CELL PROTEINS (HCPs): a MULTI-COMPANY COLLABORATIVE VIEW. *Biotechnol Bioeng*. 2021. PMID: 33930190. doi:10.1002/bit.27808
 26. Dunham WH, Mullin M, Gingras AC. Affinity-purification coupled to mass spectrometry: basic principles and strategies. *Proteomics* PMID: 22611051. 2012;12(10):1576–90. doi:10.1002/pmic.201100523.
 27. Moser AC, Hage DS. Immunoaffinity chromatography: an introduction to applications and recent developments. *Bioanalysis* PMID: 20640220. 2010;2(4):769–90. doi:10.4155/bio.10.31.
 28. Henry SM, Sutlief E, Salas-Solano O, Valliere-Douglass J. ELISA reagent coverage evaluation by affinity purification tandem mass spectrometry. *MAbs* PMID: 28708446. 2017;9(7):1065–75. doi:10.1080/19420862.2017.1349586.
 29. Pilely K, Nielsen SB, Draborg A, Henriksen ML, Hansen SWK, Skriver L, Mørtz E, Lund RR. A novel approach to evaluate ELISA antibody coverage of host cell proteins—combining ELISA-based immunocapture and mass spectrometry. *Biotechnol Prog* PMID: 32087048. 2020;36(4):e2983. doi:10.1002/btpr.2983.
 30. Pichowski PD, Petyuk VA, Orton DJ, Xie F, Moore RJ, Ramirez-Restrepo M, Engel A, Lieberman AP, Albin RL, Camp DG, et al. Sources of technical variability in quantitative LC–MS proteomics: human brain tissue sample analysis. *J Proteome Res*. 2013;12(5):2128–37. PMID: 23495885. doi:10.1021/pr301146m.
 31. Bian Y, Zheng R, Bayer FP, Wong C, Chang Y-C, Meng C, Zolg DP, Reinecke M, Zecha J, Wiechmann S, et al. Robust, reproducible and quantitative analysis of thousands of proteomes by micro-flow LC–MS/MS. *Nat Commun*. 2020;11(1):157. PMID: 31919466. doi:10.1038/s41467-019-13973-x.
 32. Sitek B, Waldera-Lupa DM, Poschmann G, Meyer HE, Stühler K. Application of label-free proteomics for differential analysis of lung carcinoma cell line A549. *Methods Mol Biol* PMID: 22665305. 2012;893:241–48. doi:10.1007/978-1-61779-885-6_16.
 33. Yuk IH, Nishihara J, Walker D, Huang E, Gunawan F, Subramanian J, Pynn AFJ, Yu XC, Zhu-Shimoni J, Vanderlaan M, et al. More similar than different: host cell protein production using three null CHO cell lines. *Biotechnol Bioeng*. 2015;112(10):2068–83. PMID: 25894672. doi:10.1002/bit.25615.
 34. Albrecht S, Kaisermayer C, Gallagher C, Farrell A, Lindeberg A, Bones J. Proteomics in biomanufacturing control: protein dynamics of CHO-K1 cells and conditioned media during apoptosis and necrosis. *Biotechnol Bioeng* PMID: 29427454. 2018;115(6):1509–20. doi:10.1002/bit.26563.
 35. Hu A, Noble WS, Wolf-Yadlina A. Technical advances in proteomics: new developments in data-independent acquisition. *F1000Res* PMID: 27092249. 2016;5:F1000 Faculty Rev–419. doi:10.12688/f1000research.7042.1.
 36. Huang L, Wang N, Mitchell CE, Brownlee T, Maple SR, Felippis MRD. A novel sample preparation for shotgun proteomics characterization of HCPs in antibodies. *Anal Chem* PMID: 28414239. 2017;89(10):5436–44. doi:10.1021/acs.analchem.7b00304.
 37. Kufer R, Haindl M, Wegele H, Wohlrab S. Evaluation of peptide fractionation and native digestion as two novel sample preparation workflows to improve HCP characterization by LC–MS/MS. *Anal Chem* PMID: 31260267. 2019;91(15):9716–23. doi:10.1021/acs.analchem.9b01259.
 38. Johnson RO, Greer T, Cejkov M, Zheng X, Li N. Combination of FAIMS, protein a depletion, and native digest conditions enables deep proteomic profiling of host cell proteins in monoclonal antibodies. *Anal Chem* PMID: 32628830. 2020;92(15):10478–84. doi:10.1021/acs.analchem.0c01175.
 39. Tjio JH, Puck TT. Genetics of somatic mammalian cells. II. Chromosomal constitution of cells in tissue culture. *J Exp Med* PMID: 13563760. 1958;108(2):259–68. doi:10.1084/jem.108.2.259.
 40. Urlaub G, Chasin LA. Isolation of Chinese hamster cell mutants deficient in dihydrofolate reductase activity. *Proc Natl Acad Sci U S A* PMID: 6933469. 1980;77(7):4216–20. doi:10.1073/pnas.77.7.4216.
 41. Popov N, Schmitt M, Schulzeck S, Matthies H. Eine störungsfreie Mikromethode zur Bestimmung des Proteingehaltes in Gewebehomogenaten. *Acta Biol Med Ger*. 1975;34:1441–46. PMID: 1221733.
 42. Weingarten P, Lutter P, Wattenberg A, Bluggel M, Bailey S, Klose J, Meyer HE, Huels C. Application of proteomics and protein analysis for biomarker and target finding for immunotherapy. *Methods Mol Med* PMID: 15585920. 2005;109:155–74. doi:10.1385/1-59259-862-5:155.